Reprinted from

EARTH AND PLANETARY SCIENCE LETTERS

Earth and Planetary Science Letters 122 (1994) 195–206

Investigation of spreading center evolution by joint inversion of seafloor magnetic anomaly and tectonic fabric data

Tom Shoberg, Seth Stein

Department of Geological Sciences, Northwestern University, Evanston, IL 60208-2150, USA

(Received August 20, 1993; revision accepted January 22, 1994)

ELSEVIER

EARTH AND PLANETARY SCIENCE LETTERS

EDITORS

F. ALBAREDE (Lyon)
U.R. CHRISTENSEN (Göttingen)
M. KASTNER (La Jolla, Calif.)
C. LANGMUIR (Palisades, N.Y.)
P. TAPPONNIER (Paris)
R. VAN DER VOO (Ann Arbor, Mich.)

ADVISORY EDITORIAL BOARD

Australia
K. LAMBECK (Canberra, A.C.T.)

Belgium
A.L. BERGER (Louvain-La-Neuve)

France
C.J. ALLÈGRE (Paris)
Y. BOTTINGA (Paris)
J.P. COGNÉ (Paris)
V. COURTILLOT (Paris)
C. JAUPART (Paris)
H.C. NATAF (Paris)

Germany
H. PALME (Mainz)
S.L. GOLDSTEIN (Mainz)

India
S. KRISHNASWAMI (Ahmedabad)

Israel
J.R. GAT (Rehovot)

Italy
A. LONGINELLI (Trieste)

People's Republic of China
TU GUANGZHI (Guiyang)

United Kingdom
J.C. BRIDEN (Swindon)
N.J. KUSZNIR (Liverpool)
R.K. O'NIONS (Cambridge)

U.S.A.
W.S. BROECKER (Palisades, N.Y.)
J.M. EDMOND (Cambridge, Mass.)
A.N. HALLIDAY (Ann Arbor, Mich.)
J.L. KIRSCHVINK (Pasadena, Calif.)
D. LAL (La Jolla, Calif.)
J.G. SCLATER (La Jolla, Calif.)
N.H. SLEEP (Stanford, Calif.)
S. UYEDA (College Station, Tex.)

EDITORIAL ADDRESSES

Dr. F. Albarède
Ecole Normale Supérieure de Lyon
46 Allée d'Italie,
69364 Lyon Cedex 07, France
Tel.: (33) 72728414
Fax: (33) 72728080
E-mail albarede@geologie.ens-lyon.fr

Prof. M. Kastner
Geological Research Division
Scripps Institution of Oceanography
University of California
La Jolla, CA 92093, U.S.A.
Tel.: (619) 534-2065/Fax: (619)534-0784
INTERNET: m.kastner@ucsd.edu

Dr. P. Tapponnier
Institut de Physique du Globe
Mécanique Matériaux Terrestres
4 place Jussieu, Tour 24, 2ème etage,
75230 Paris Cédex 05, France
Tel.: (44) 273905
Fax: (44) 273373

Dr. U.R. Christensen
Institut für Geophysik
Universität Göttingen
Herzberger Landstrasse 180
D-3400 Göttingen, Germany
Tel.: (551) 397 451
Fax: (551) 397 459

Prof. C. Langmuir
Lamont-Doherty Geological Observatory
of Columbia University
Palisades, NY 10964-0190, U.S.A.
Tel.: (914) 359-2900/Fax: (914) 365-3183
E-mail: langmuir@ldeo.colombia.edu

Dr. R. van der Voo
University of Michigan,
Department of Geological Sciences,
1006 C.C. Little Building,
Ann Arbor, MI 48109-1063, U.S.A.
Tel.: (313) 764 1435
Fax: (313) 763 4690

PUBLICATION INFORMATION

Earth and Planetary Science Letters (ISSN 0012-821X). For 1994 volumes 120–126 are scheduled for publication. Subscription prices are available upon request from the publisher. Subscriptions are accepted on a prepaid basis only and are entered on a calendar year basis. Issues are sent by surface mail except to the following countries where air delivery via SAL is ensured: Argentina, Australia, Brazil, Canada, Hong Kong, India, Israel, Japan, Malaysia, Mexico, New Zealand, Pakistan, PR China, Singapore, South Africa, South Korea, Taiwan, Thailand, USA. For all other countries airmail rates are available upon request. Claims for missing issues must be made within six months of our publication (mailing) date. Please address all your requests regarding orders and subscription queries to: Elsevier Science B.V., Journal Department, P.O. Box 211, 1000 AE Amsterdam, The Netherlands. Tel.: 31-20-5803642, fax: 31-20-5803598. *U.S. mailing notice: Earth and Planetary Science Letters* (ISSN 0012-821X) is published monthly by Elsevier Science B.V., Molenwerf 1, P.O. Box 211, 1000 AE, Amsterdam, The Netherlands. The annual subscription price in the U.S.A. is ca. U.S. $1366 (US$ price valid in North, Central and South America only) including air-speed delivery. Second class postage paid at Jamaica, NY 11431, U.S.A. *U.S.A. postmasters:* Send address changes to *Earth and Planetary Science Letters*, Publications Expediting, Inc., 200 Meacham Avenue, Elmont, NY 11003, U.S.A.

© 1994, ELSEVIER SCIENCE B.V. ALL RIGHTS RESERVED

0012-821X/94/$07.00

No part of this publication may be reproduced, stored in a retrieval system or transmitted in any form or by any means, electronic, mechanical, photocopying, recording or otherwise, without the prior written permission of the publisher. Elsevier Science B.V., Copyright & Permissions Department, P.O. Box 521, 1000 AM Amsterdam, The Netherlands.
Upon acceptance of an article by the journal, the author(s) will be asked to transfer copyright of the article to the publisher. The transfer will ensure the widest possible dissemination of information.
Special regulations for readers in the USA – This journal has been registered with the Copyright Clearance Center, Inc. Consent is given for copying of articles for personal or internal use, or for the personal use of specific clients. This consent is given on the condition that the copier pays through the Center the per-copy fee stated in the code on the first page of each article for copying beyond that permitted by Sections 107 or 108 of the US Copyright Law. The appropriate fee should be forwarded with a copy of the first page of the article to the Copyright Clearance Center, Inc., 27 Congress Street, Salem, MA 01970, USA. If no code appears in an article, the author has not given broad consent to copy and permission to copy must be obtained directly from the author. *The fee indicated on the first page of an article in this issue will apply retroactively to all articles published in the journal, regardless of the year of publication.* This consent does not extend to other kinds of copying, such as for general distribution, resale, advertising and promotion purposes, or for creating new collective works. Special written permission must be obtained from the publisher for such copying.
No responsibility is assumed by the Publisher for any injury and/or damage to persons or property as a matter of products liability, negligence or otherwise, or from any use or operation of any methods, products, instructions or ideas contained in the material herein.
Although all advertising material is expected to conform to ethical (medical) standards, inclusion in this publication does not constitute a guarantee or endorsement of the quality or value of such products or of the claims made of it by its manufacturer.

This issue is printed on acid-free paper.

Printed in the Netherlands

ELSEVIER

Earth and Planetary Science Letters 122 (1994) 195–206

EPSL

Investigation of spreading center evolution by joint inversion of seafloor magnetic anomaly and tectonic fabric data

Tom Shoberg, Seth Stein

Department of Geological Sciences, Northwestern University, Evanston, IL 60208-2150, USA

(Received August 20, 1993; revision accepted January 22, 1994)

Abstract

Spreading center segments that have experienced a complex tectonic history including rift propagation may have a complicated signature in bathymetric and magnetic anomaly data. To gain insight into the history of such regions, we have developed techniques in which both the magnetic anomaly patterns and seafloor fabric trends are predicted theoretically, and the combined predictions are compared numerically with the data to estimate best fitting parameters for the propagation history. Fitting functions are constructed to help determine which model best matches the digitized fabric and magnetic anomaly data. Such functions offer statistical criteria for choosing the best fit model. We use this approach to resolve the propagation history of the Cobb Offset along the Juan de Fuca ridge. In this example, the magnetic anomaly data prove more useful in defining the geometry of the propagation events, while the fabric, with its greater temporal resolution, is more useful for constraining the rate of propagation. It thus appears that joint inversion of magnetic and seafloor fabric data can be valuable in tectonic analyses.

1. Introduction

Considerable attention has been focused in recent years on areas along mid-ocean ridges whose geometry has evolved in a manner more complex than simple ridge-transform systems. These regions vary in size from discrete microplates [1–10], to propagating rifts [11–14], overlapping spreading centers (OSCs) [15], and smaller along-axis discontinuities known variously as 'saddle points' [16], 'devals' [17], or 'SNOOs' [18]. These features can cause significant variations in spreading geometry along-strike, which, in turn, may reflect the dynamics of magmatic accretion between and along ridge segments [19–22].

The larger of these systems, microplates, propagators and OSCs, have a discrete region of lithosphere between two overlapping ridge segments. Commonly, a propagating rift segment (Fig. 1) lengthens at the expense of an adjacent doomed rift segment, which is pre-empted and eventually ceases spreading. The locus of relative motion between the two plates shifts from the doomed rift to the propagating one, transferring lithosphere from one plate to the other. This process leaves a distinctive signature in the magnetic anomalies, tectonic fabric and bathymetry of the seafloor associated with the overlap. The boundaries between lithosphere formed at the propagating rift and the pre-existing lithosphere are age discontinuities, called pseudofaults, which are

[MK]

0012-821X/94/$07.00 © 1994 Elsevier Science B.V. All rights reserved
SSDI 0012-821X(94)00024-S

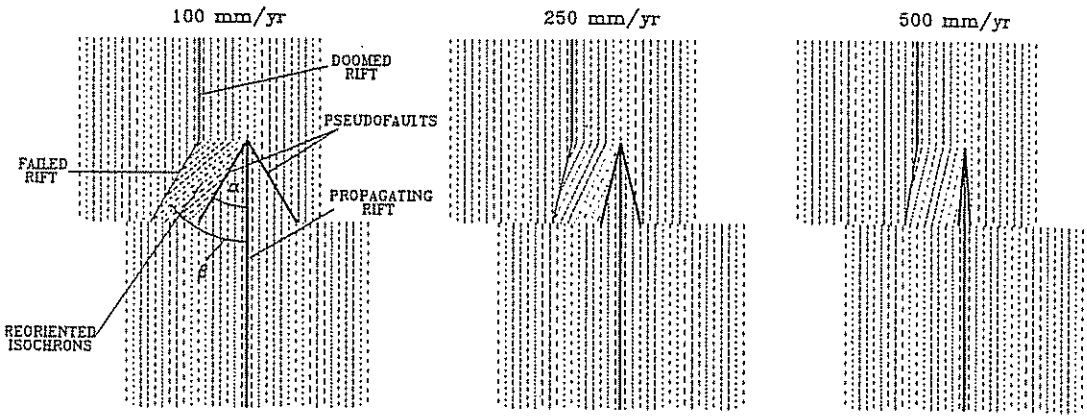

Fig. 1. Pseudofault and isochron configuration for a simple propagating rift geometry as a function of propagation rate. The pseudofaults are the thick solid lines forming the arrowhead patterns at the tip of the lower rift, the isochrons are represented by thin dashed lines, and the thin solid lines represent failed rifts. The angle between the pseudofault and the propagating rift (α) decreases as the propagation rate increases, as does the isochron reorientation angle (β).

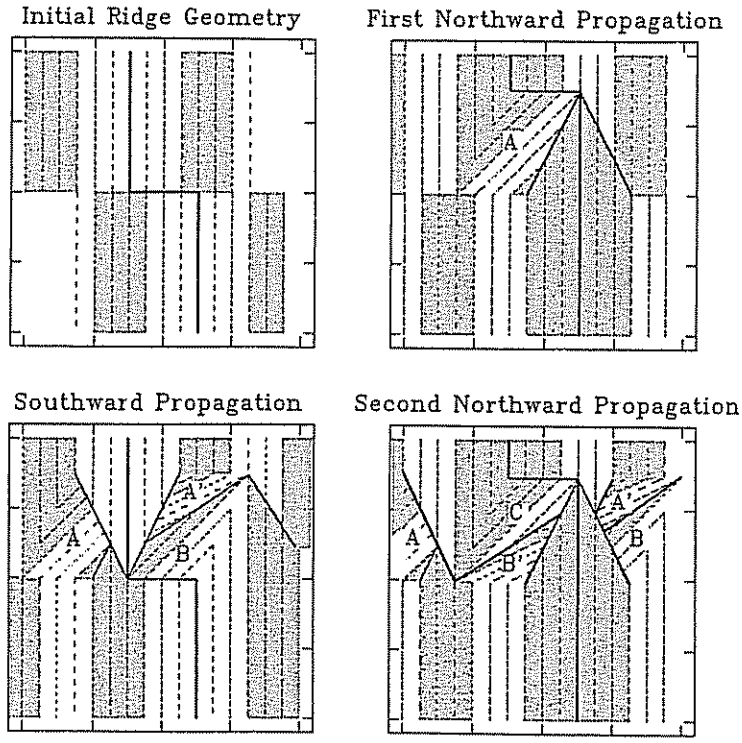

Fig. 2. Predicted fabric and pseudofault orientation from a dueling propagator model with three stages. White and stippled regions = alternating normal and reverse polarity magnetic anomalies; thick solid lines = pseudofaults and active rifts; thin dashed lines = isochrons. The reoriented isochrons, magnetic anomalies and pseudofaults show a complex pattern with five different domains (A, A', B, B' and C).

oblique to both the ridge segments and the transform fault connecting the rift tips. As the transform fault migrates, lithosphere is transferred from one plate to the other, so originally ridge-parallel isochrons formed prior to the arrival of the propagating rift tip are reoriented and become oblique features.

Pseudofaults, magnetic anomalies and seafloor fabric oblique to both the spreading direction and ridge trend are thus primary diagnostics of propagating rift systems. By assuming that the magnetic anomalies and seafloor fabric represent isochrons, it is possible to model the kinematics of the rift propagation process. In the simplest case, where the propagating and doomed rifts are parallel, the angle, α, between the pseudofaults and the propagating rift is related to the half-spreading rate, u, and the propagation rate, w: $\alpha = \tan^{-1}(u/w)$. Similarly, the angle β between an isochron before and after it was rotated (taken as positive clockwise) depends on the ratio of the two rates: $\beta = \tan^{-1}(2u/w)$. Thus, for a given spreading rate, more rapid propagation gives rise to a narrower wedge of lithosphere between the pseudofaults and propagating ridge and to less reorientation of the isochrons.

This simple propagation model can be generalized to more complex models for the evolution of the region between the ridge segments. For example, in 'dueling propagator' systems, propagation events repeatedly alternate between two ridge segments and each grows at the expense of the other [22,23]. Isochrons that are caught within these dueling ridges are reoriented on each pass of the active spreading center (Fig. 2). Thus successive propagation events lead to more oblique orientations.

For this simple case, with three propagation events, each occurring with a propagation rate equal to the full spreading rate, the reoriented fabric, pseudofaults and magnetic anomalies show a complex pattern with five different domains. The isochrons and magnetic anomalies in regions A′ and B′ have been twice reoriented and the pseudofaults separating the primed from the unprimed regions have also been reoriented. Therefore, apparent propagation rates inferred from these orientations would be inaccurate [24].

Magnetic anomaly patterns depend on the amount of crust transferred between plates. This transfer produces complex and asymmetric magnetic anomaly patterns which depend on the propagating ridge geometry. In particular, some patches of crust formed during the same polarity chron are split and separated by rift propagation, making it difficult to infer their age. Such areas are wider or narrower than coeval patterns outside the propagation area. As a result, it can be difficult to estimate spreading rates from these patterns, making determining the tectonic history of such a region challenging.

2. The inverse problem

Due to the fact that the magnetic anomaly and seafloor tectonic fabric provide the primary constraints on the rift propagation process, we can treat modeling the evolution of such areas as an inverse problem. We seek to find a spreading center history that best predicts the present magnetic anomaly and seafloor fabric configuration. The forward problem, predicting isochrons from a seafloor spreading history, is conceptually straightforward, although complicated for a complex spreading history. The inverse problem is more difficult. The isochrons available for this purpose are interpreted from two data types: magnetic anomalies and seafloor fabric. Each data set has its advantages and limitations.

Magnetic anomaly lineations, the traditional data source, provide suitable isochrons to infer the propagation history, provided the region between the ridge segments is large enough that its tectonic evolution requires a time period spanning magnetic polarity reversals. If, however, the region is small, much of the lithosphere formed at either ridge during the propagation history may have formed within a single magnetic polarity interval. In this case no magnetic boundary separates the lithosphere formed on the two ridges, so magnetic anomalies and pseudofaults are difficult to identify. A further complexity is that the relation between magnetic polarity and age can be complicated. For a simple case in which the ridge geometry does not change, suc-

cessive polarity regions at increasing distance from the ridge are easily assigned ages from the reversal sequence. In a complicated case, however, the transfer of material between plates can make it difficult to assign an age to lithosphere of a particular polarity.

In recent years acoustic imaging systems have provided a second data set: seafloor lineations or tectonic fabric [e.g., 12]. Such fabric, like magnetic anomaly lineations, appears to form near the ridge axis and retain this trend as it moves away from the ridge. We thus assume that fabric can be generally treated as isochrons, although there are clearly other processes that can give lineations that are not isochrons. The fabric differs from the magnetic lineations in that it contains no specific age information, so individual lineations cannot be matched with others, as is possible with magnetic data. Their advantage, however, is that they are produced more frequently than the magnetic isochrons, which are visible only at reversal boundaries. Hence, although all lithosphere produced during the current magnetic polarity chron (730,000 yr) has the same magnetic polarity, and thus no identifiable isochrons within it, seafloor lineations are identifiable within this age range. For example, the fabric in the Cobb Offset region has a mean age

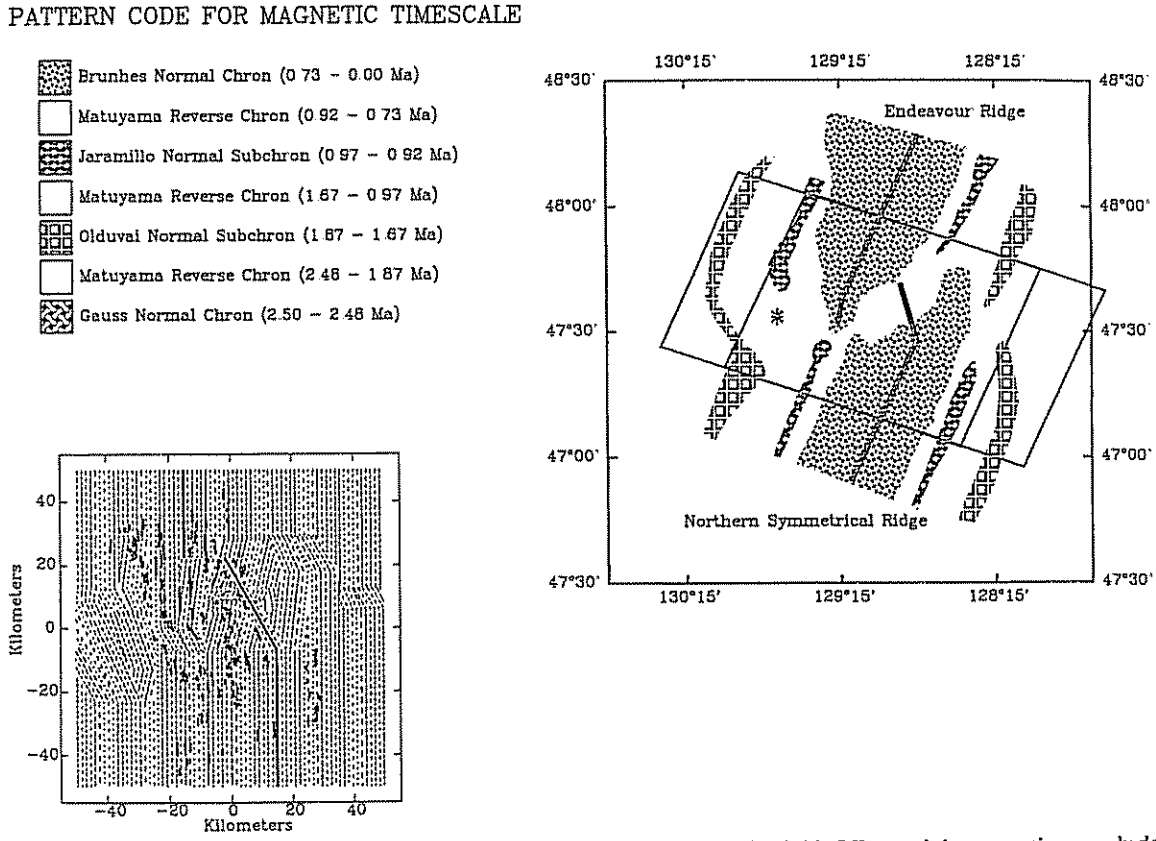

Fig. 3. Location of data used in this study. Upper right panel shows the location of the Cobb Offset and the magnetic anomaly data [22]. The large and small boxes represent the areas for which we modeled the magnetic anomalies and seafloor fabric, respectively. The asterisk shows area of anomalously wide reversely magnetized lithosphere as noted by Johnson et al. [22]. The patterns associated with magnetic anomalies are shown in the upper left. The lower left shows a comparison of the digitized observed seafloor fabric data (thick solid lines) with the synthetic isochrons (thin dashed lines), using the best fitting propagation rate (500 mm/yr) [after 24]. In this panel and Fig. 4 the figures are centered at 47.54°N, 129.07°W and rotated such that N22°E is toward the top of the page.

spacing of 141,000 ± 91,300 yr (uncertainty is one standard deviation).

In a previous study [24], we showed that isochrons generated for a dueling propagator model of the Cobb Offset region of the Juan de Fuca Ridge could be matched to seafloor fabric data. We treated the isochrons as synthetic tectonic fabric and generated such fabric for a variety of propagation rates. Numerical comparison of the fit between the observed lineations and models provided an objective estimate of the propagation rate that best fit the data set as a whole, and its associated uncertainty. Thus, we were solving the inverse problem of finding the propagation rate by solving the forward problem for a range of model parameters, and finding the best fit. This approach is common for inverse problems like this, in which the forward problem is not easy to invert formally.

Our goal here is to extend this technique to a joint inversion of magnetic anomaly and seafloor fabric data. Because the two data types have distinct strengths and weaknesses, each can contribute differently to a joint solution. We apply this technique to the Cobb Offset region, building on our previous fabric study [24].

3. The Cobb Offset, Juan de Fuca Ridge

The geometry of the Juan de Fuca Ridge, separating the Pacific and Juan de Fuca plates, has evolved through most of the Tertiary by rift propagation [11,25–27,22,28–31]. The Cobb Offset, at about 47.5°N, 129°W, separates the Northern Symmetrical Ridge (NSR) segment from the Endeavour segment. Currently, the two ridge segments overlap for about 30 km, and are separated by about 30 km in the overlap region. For convenience, we use the term 'overlap' without implying that the overlapping ridge segments spread simultaneously.

A striking feature of the magnetic anomaly data (Fig. 3) is the area, formed during the Brunhes normal chron, composed of two wedge-shaped regions; one southward pointing on the Endeavour segment and one northward pointing on the NSR segment. Hey and Wilson [27] interpreted the wedge boundaries as pseudofaults indicating northward rift propagation. Johnson et al. [22] inferred, from an anomalously wide zone of reversely magnetized crust adjacent to the Olduvai anomaly on the Pacific side (asterisk in Fig. 3), that an earlier propagation episode occurred before that indicated by the tapered Brunhes anomaly. They also used the locations of fresh basalts to infer that the locus of active spreading on the NSR trends northwesterly from the center of the region of Brunhes normal crust. A subsequent Seabeam study [29] also supports this interpretation. In this model the propagating NSR tip does not bisect the wedge of Brunhes-age crust and has no observable magnetic anomaly signature, presumably because it started spreading only very recently.

To explain the series of propagation events, Johnson et al. [22] proposed a dueling propagator model in which northward and southward propagation events alternated, with only one of the overlapping ridges active at any given time. In our earlier study, we parameterized this model and found that it worked well [24], we thus use this parameterization in the present study.

4. Fabric fitting

In studying the fabric we use the approach and data set from our earlier study [24], consisting of 154 lineations digitized from a SeaMARC imagery map [32], which are described by position and trend. The lineations were chosen because they appear not to have been affected by extraneous volcanism, such as a seamount. These fabric elements range from 2 to 15 km in length and are less than 0.5 km wide. An important feature of the data is the large number of fabric elements within the overlap region. These are oblique to the trends of the boundaries between polarity chrons, except where chrons are truncated by pseudofaults. The most useful constraint on the propagation models comes from fabric oriented approximately NE–SW, which appear to have been reoriented by propagation. The current positions of the ridge segments are taken from the bathymetry [29].

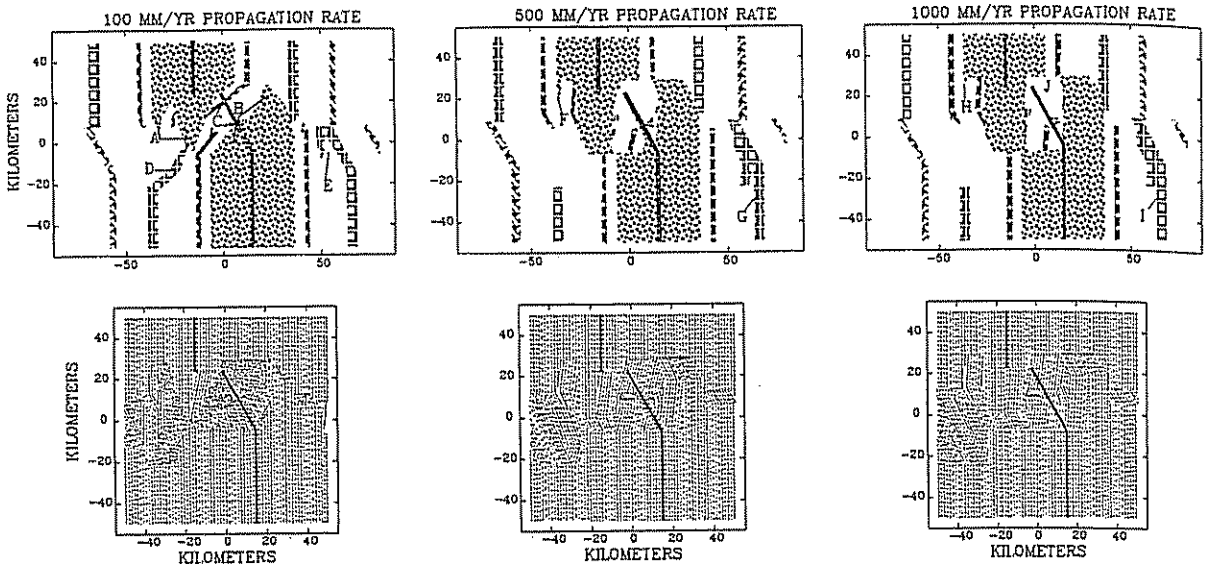

Fig. 4. Magnetic anomaly and seafloor lineation predictions for models with propagation rates of 100 mm/yr (left), 500 mm/yr (center), and 1000 mm/yr (right). Magnetic isochron patterns are the same as in Fig. 3. Letters labeling regions in upper panels are discussed in the text.

The fabric data are compared with synthetic isochrons predicted by the Johnson et al. [22] rift propagation history, with minor modifications to fit the magnetic anomaly data better [24]. We assume the simplest possible propagator kinematics, in which spreading is instantaneously transferred from the doomed to the propagating ridge and neither a microplate nor a shear zone forms. We use a time step of 10,000 yr and generate synthetic isochrons every 50,000 yr, so events of duration of less than a few thousand years are not visible in the models.

For this propagation history, we test the effect of rift propagation rates at 100 mm/yr increments between 100 and 1000 mm/yr. Propagation rates less than 100 mm/yr were excluded by the magnetic anomaly data because insufficient lithosphere would be formed. All of the models fit the major bathymetric features well. Three statistical measures: number of fabric elements misfit, number well fit, and percentage well fit, were used to quantify the model fit. A fabric element is considered well fit if the predicted trend is within 15° of the observed trend and misfit if the predicted trend is misaligned by more than 30°.

It is unclear which test serves best, but all yield similar information. Models with rates ranging from 400 to 800 mm/yr are indistinguishable, whereas lower rates have clearly poorer fits. For a reduced χ^2 test, propagation rates from 500 to 900 mm/yr were indistinguishable at the 99% confidence level.

Fig. 5. Use of the different fitting functions to compare predicted seafloor fabric and magnetic anomalies with the digitized data, as a function of propagation rate. Left box in each row represents the number of data misfit, the center box represents the number of data well fit and the right box represents the percentage of the data well fit. Top row = fits to the fabric data; second row = fits to the magnetic anomaly data using the isochron criterion; third row = fits to the magnetic anomaly data using the polarity criterion; fourth row = additive combination of the fabric and magnetic anomaly polarity results; fifth row = scaled combination of the fabric and magnetic anomaly polarity results; bottom row = weighted combination of the fabric and magnetic anomaly polarity results.

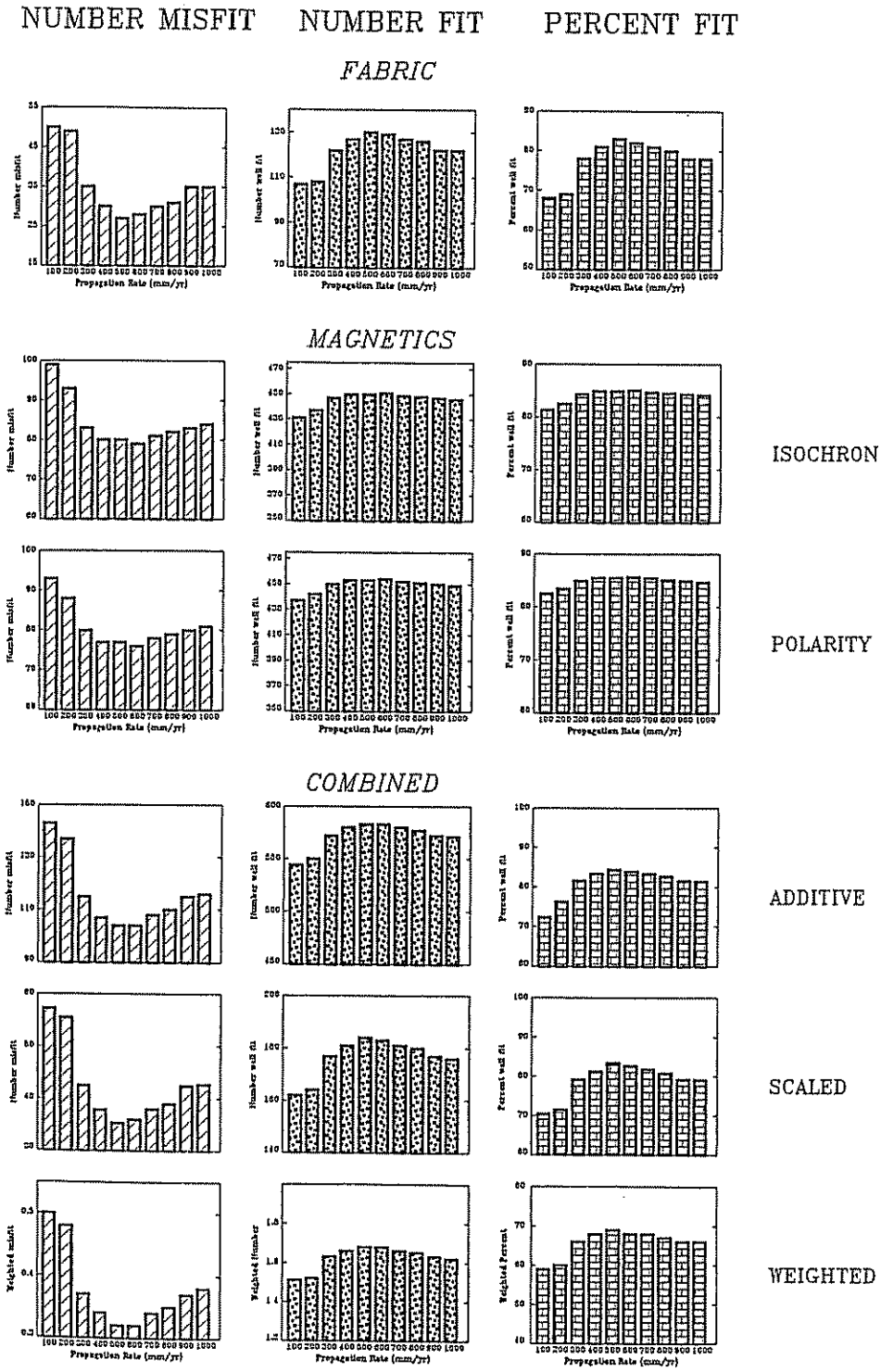
NUMBER MISFIT
NUMBER FIT
PERCENT FIT
FABRIC
MAGNETICS
COMBINED
ISOCHRON
POLARITY
ADDITIVE
SCALED
WEIGHTED

5. Magnetic anomaly fitting

To complement the seafloor fabric study, we need the magnetic anomalies in digital form to test for agreement between the model predictions and the observations. Previous magnetic anomaly modeling used polarity block models to match contoured magnetic anomaly data [22,24] and so were not able to resolve propagation rates. We digitized the magnetic anomaly patterns of Johnson et al. [22] on 5 km wide grid and compared the resulting 530 data points with the predictions from the models. These data are described by position and either polarity or chron number.

As in the fabric study, we iterated over propagation rates from 100 to 1000 mm/yr. We compared the model predictions with the digitized data using two different misfit criteria. The first, a polarity criterion, considers data misfit when the polarity of the predicted magnetic anomaly is opposite to that observed. In the other criterion, which we call an isochron criterion, data are considered misfit if the predicted chrons and subchrons do not match those interpreted by Johnson et al. [22]. This second criterion is more stringent in that it requires correct age assessments for each chron. The price of this stringency is a model dependence in interpreting chrons and subchrons for the magnetic anomalies. This can be difficult for regions with complicated magnetic anomaly patterns resulting from a dueling propagator history.

Magnetic anomaly predictions for three of the models (100, 500 and 1000 mm/yr) are shown in Fig. 4. Numerical comparison with the magnetic anomaly data (Fig. 3) shows the fit and misfit regions. The major misfits for the 100 mm/yr model are the wider than observed Brunhes normal region (left region labeled A, and those labeled B), a thinner than observed Brunhes normal region (right region labeled A), the Jaramillo event in the overlap zone (C), and the Olduvai chrons labeled D and E. The major misfits for the 500 mm/yr model occur in a Brunhes-aged wedge (F) and the thinner than observed Olduvai aged lithosphere (G). The misfits in the 1000 mm/yr model are mainly in the same areas as the 500 mm/yr model (H and I) and in a thinner than observed Matuyama section in the overlap zone (J).

Numerical measures of model fit are shown in Fig. 5. For both the polarity and isochron misfits we compute the number of points misfit, number of points well fit and percentage of points well fit. Although the variations between the fits of the magnetic anomaly models with different propagation rates are smaller than those for the fabric, the shape of the histograms are similar. This agreement is gratifying in that it shows the consistency of the data sets. Hence, by digitizing the magnetic anomalies we can numerically constrain the propagation rate, whereas analog comparisons with block models could only say that this rate was high. Consequently, the numerical magnetic anomaly modeling alone constrains the rift propagation rates, even though such modeling has a much coarser temporal resolution than the fabric modeling.

6. Joint fitting

Due to the fact that the magnetic anomaly and the seafloor fabric data both contain information about the history of the dueling propagator system, it seemed natural to fit the two data sets jointly. We constructed fitting functions to combine the seafloor fabric fits, which have a continuous quality of fit (the angle between the predicted and the observed trends), with the magnetic anomaly fits, which are binary in nature (points are either well fit or misfit). Using these definitions of well fit and misfit has the advantage of permitting direct combination of the data sets into a single fitting function, but the disadvantage of making it difficult to use standard statistical techniques to estimate confidence limits.

We use three fitting functions to combine the magnetic anomaly polarity and seafloor fabric fits:

(1) Additive combination of fits, misfits and percentages. For example:

Combined fit

= *Number of fabric elements well fit*

+ *Number of magnetic points well fit*

(2) Scaled combination. The magnetic anomaly data are sampled more coarsely and over a larger scale than the fabric data. Therefore, we used a scaling factor, based on grid size, to reduce this bias:

Scaled combination

$$= \tfrac{5}{6} \times (\textit{fabric data well fit}) + \tfrac{1}{6} \times (\textit{magnetic data well fit})$$

(3) Weighted combinations. Both the fabric and magnetic fits are divided by the total number of points associated with each respectively:

Weighted combination

$$= \frac{\textit{number of fabric data misfit}}{\textit{total number of fabric data}} + \frac{\textit{number of magnetic data misfit}}{\textit{total number of magnetic data}}$$

Histograms showing the number of data misfit, and the number and percentage of data well fit for the additive combination of the magnetic anomaly and seafloor fabric data are presented in the fourth row of Fig. 5. Those for the scaled combinations are presented in the fifth row, and those for the weighted combinations are presented in the bottom row. The three methods produce curves of approximately the same shape, which is not surprising as fits to the magnetic anomalies and the seafloor fabric individually both show similar shapes. We feel that the similarity of shape for each of the fitting functions implies that the estimate of the propagation rate is robust. The best fit rate in all these tests was 500–600 mm/yr.

Both the fabric and magnetic anomaly data, and hence combinations of the two, have better resolution for the low propagation rates than for the higher ones. Relative to the preferred rate

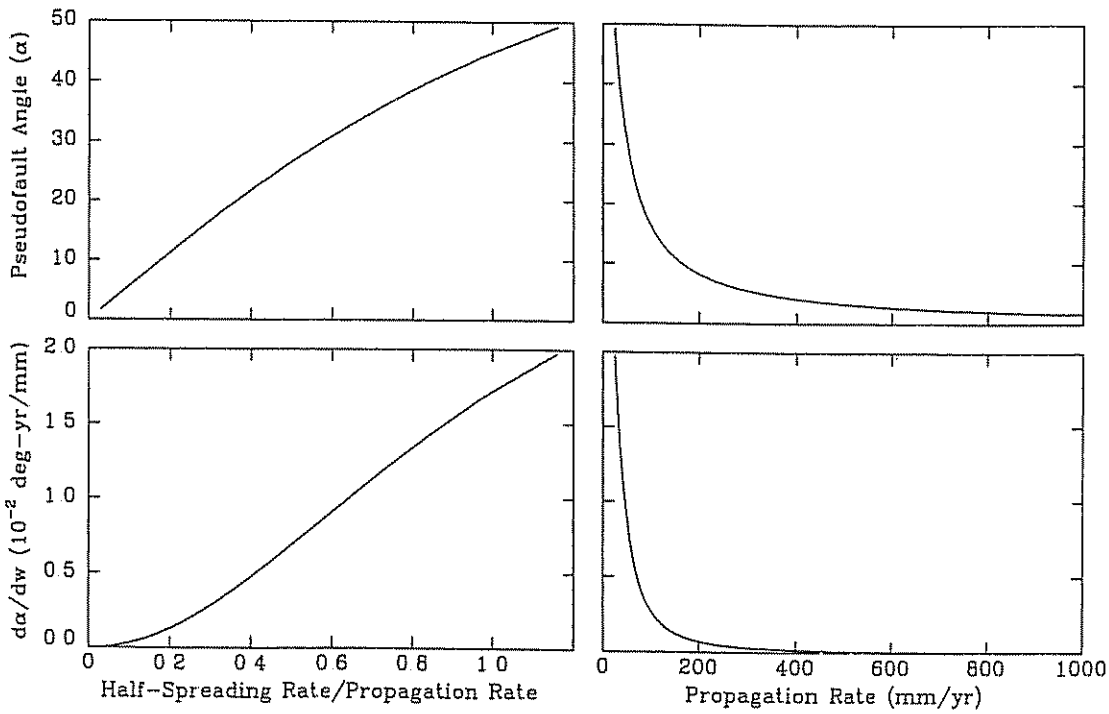

Fig. 6. Variation of pseudofault angle and its rate of change with respect to propagation rate. The upper left panel is a plot of the pseudofault angle as a function of the ratio of the half-spreading rate to the propagation rate. The lower left panel is a plot of the rate of change of this angle with respect to propagation rate versus the same ratio. The right hand panels show the same respective dependent variables plotted against propagation rate. In all cases the half-spreading rate is 29 mm/yr.

(500–600 mm/yr) the rates that are too slow are worse fit than those which are too high. This is because of the way the pseudofault and reoriented lineation angles depend on the propagation rate. The derivative of the pseudofault angle, α, with respect to the propagation rate w is $d\alpha/dw = -u/(w^2+u^2)$. As shown in Fig. 6, for the Cobb Offset half-spreading rate ($u = 29$ mm/yr), the rate of change of the pseudofault angle approaches its asymptotic limit where the propagation rate exceeds 300 mm/yr, or, equivalently, the ratio of half-spreading rate to propagation rate is less than 0.1. Thus, in this case, even large changes in propagation rates produce only minor changes in the pseudofault angle. The reoriented lineations behave similarly.

6. Discussion

We find that digitized magnetic anomaly and seafloor fabric data provide consistent and complementary constraints on rift propagation models. As expected, the seafloor fabric, with its finer temporal resolution, provides a stronger constraint on the propagation rate. The magnetic anomaly data also constrain the propagation rate, but their contribution is largely to constrain the history of the spreading rates and propagation events. Because the latter constraints are fixed throughout our modeling, the contribution of the magnetic anomaly data is greater than implied by our fitting functions.

The results for the Cobb Offset support our suggestion [24] that rates of propagation over the past 2 Myr were rapid. Fast propagation rates have been found in detailed studies along sections of the East Pacific Rise [e.g., 10,33] and it seems likely that further detailed studies will be able to resolve propagation rates better, particularly for dueling propagator systems.

We thus feel that joint numerical fitting of seafloor magnetic anomaly and fabric data has the potential to be a valuable tool for studying spreading center evolution. The results illustrate that best fitting tectonic history models can be derived using objective criteria, and that confidence limits on key parameters can be estimated. It should be noted that both our modeling approach, and the earlier modeling studies, implicitly make use of results in addition to those from the magnetic and fabric data. The Cobb models, for example, use dredging and Seabeam results to locate the propagating NSR tip, which is not visible in the magnetic data.

The success of our simple analysis of this inverse problem suggests several approaches that may make this technique more useful.

First, such a joint analysis can be used to solve for more than the rift propagation rate alone. Conceptually, there is no reason why both the spreading history and propagation geometry cannot be estimated in the same way. The fabric data alone do not constrain the spreading rates independently of the propagation rates and only weakly constrain the propagation geometry. Digital fitting of the magnetic anomaly data, however, should be quite valuable for these purposes, so long as the propagation events span more than one polarity chron. For the Cobb Offset, our analysis showed that the propagation history determined in the earlier magnetic studies was quite good, and needed only minor refinement. In less well studied situations it may be necessary to determine more than the propagation rate alone.

Second, our technique might be improved by more sophisticated joint fitting functions. Our experiments with simple fitting functions find quite robust results for the Cobb Offset. The primary question, of course, is how to estimate best the joint best fit of, and confidence limits for, the magnetic and fabric models. The 'common sense' joint fitting functions we use adequately estimate the best fit propagation rate. They do not, however, provide confidence limits, because the fit to the magnetic data is binary, whereas the fabric fit is continuous.

Third, the analysis could be made easier and more objective by working directly from digital data rather than from analog images. Recent results with bathymetric and side-scan data [34] illustrate the potential for identifying and characterizing lineations directly. Similarly, it would be desirable to work with digital magnetic anomaly data rather than analog patterns.

Finally, other data may also be useful in fur-

ther constraining such models. For example, propagating rift tips have been associated with particularly strong magnetic intensities [e.g., 35,33], which could be used to constrain rift tip locations. It may also be possible to include seafloor depth data, which might discriminate different aged blocks of the same magnetic polarity that have been juxtaposed.

7. Acknowledgements

We thank Mark T. Woods for helpful discussions, Jeffrey Karson and an anonymous reviewer for thoughtful and helpful reviews of the manuscript. This research was supported by NSF grants OCE-9019572 and EAR-9022476, and NASA grant NAG-5-1944.

8. References

[1] D.W. Forsyth, Mechanisms of earthquakes and plate motions in the East Pacific, Earth Planet. Sci. Lett. 17, 189–193, 1972.

[2] E.M. Herron, Two small crustal plates in the South Pacific near Easter Island, Nature Phys. Sci. 240, 35–37, 1972.

[3] R.N. Anderson, D.W. Forsyth, P. Molnar and J. Mammerickx, Fault plane solutions of earthquakes on the Nazca plate boundaries and the Easter plate, Earth Planet. Sci. Lett. 24, 188–202, 1974.

[4] D.W. Handschumacher, R.H. Pilger, Jr., J.A. Foreman and J.F. Campbell, Structure and evolution of the Easter plate, in: Nazca plate: Crustal Formation and Andean Convergence, L.D. Kulm, J. Dymond, E.J. Dasch and D.M. Hussong, eds., Geol. Soc. Am. Mem. 154, 63–76, 1981.

[5] J.F. Engeln and S. Stein, Tectonics of the Easter plate, Earth Planet. Sci. Lett. 68, 259–270, 1984.

[6] J.-G. Schilling, H. Sigurdsson, A.N. Davis and R.N. Hey, Easter microplate evolution, Nature 317, 325–331, 1985.

[7] S. Anderson-Fontana, J.F. Engeln, P. Lundgren, R.L. Larson and S. Stein, Tectonics and evolution of the Juan Fernandez microplate at the Pacific–Nazca–Antarctic triple junction, J. Geophys. Res. 91, 2005–2018, 1986.

[8] J.F. Engeln, S. Stein, J. Werner and R. Gordon, Microplate and shear zone models for oceanic spreading center reorganizations, J. Geophys. Res. 93, 2839–2856, 1988.

[9] R.C. Searle, R.I. Rusby, J. Engeln, R.N. Hey, J. Zukin, P.M. Hunter, T.P. LeBas, H.-J. Hoffman and R. Livermore, Comprehensive sonar imaging of the Easter micro-plate, Nature 341, 701–705, 1989.

[10] D.F. Naar and R.N. Hey, Tectonic evolution of the Easter microplate, J. Geophys. Res. 96, 7961–7993, 1991.

[11] R. Hey, A new class of "pseudofaults" and their bearing on plate tectonics: A propagating rift model, Earth Planet. Sci. Lett. 37, 321–325, 1977.

[12] R.C. Searle and R.N. Hey, Gloria observations of the propagating rift at 95.5°W on the Cocos–Nazca spreading center, J. Geophys. Res. 88, 6433–6448, 1983.

[13] D.F. Naar and R.N. Hey, Fast rift propagation along the East Pacific Rise near Easter Island, J. Geophys. Res. 91, 3425–3438, 1986.

[14] G. Acton, S. Stein and J. Engeln, Formation of curved seafloor fabric by changes in rift propagation velocity and spreading rate: Application to the 95.5°W Galapagos propagator, J. Geophys. Res. 93, 11845–11861, 1988.

[15] K.C. Macdonald and P.J. Fox, Overlapping spreading centres: New accretion geometry on the East Pacific Rise, Nature 302, 55–58, 1983.

[16] K.C. Macdonald, D. Castillo, S. Miller, P.J. Fox, K. Kastens and E. Bonatti, Deep-tow studies of the Vema fracture zone, 1, tectonics of a major slow slipping transform fault and its intersection with the Mid-Atlantic ridge, J. Geophys. Res. 91, 3334–3354, 1986.

[17] C.H. Langmuir, J.F. Bender and R. Batiza, Petrologic and tectonic segmentation of the East Pacific Rise 5°30′–14°30′N, Nature 322, 422–429, 1986.

[18] R. Batiza and S.H. Margolis, Small non-overlapping offsets of the East Pacific Rise, Nature 320, 439–441, 1986.

[19] H. Schouten, K.D. Klitgord and J.A. Whitehead, Segmentation of mid-ocean ridges, Nature 317, 225–229, 1985.

[20] H. Schouten, J.B. Dick and K.D. Klitgord, Migration of mid-ocean ridge volcanic segments, Nature 326, 835–839, 1987.

[21] J. Lin, G.M. Purdy, H. Schouten, J.C. Sempere and C. Zervas, Evidence from gravity data for focused magmatic accretion along the Mid-Atlantic Ridge, Nature 344, 627–632, 1990.

[22] H.P. Johnson, J.L. Karsten, J.R. Delaney, E.E. Davis, R.G. Currie and R.L. Chase, A detailed study of the Cobb offset of the Juan de Fuca Ridge: Evolution of a propagating rift, J. Geophys. Res. 88, 2297–2315, 1983.

[23] K.C. Macdonald, R.M. Haymon, S.P. Miller, J.-C. Sempere and P.J. Fox, Deep-Tow and Sea Beam studies of dueling propagating ridges on the East Pacific Rise near 20° 40′S, J. Geophys. Res. 93, 2875–2898, 1988.

[24] T. Shoberg, S. Stein and J. Karsten, Constraints on rift propagation history at the Cobb Offset, Juan de Fuca Ridge, from numerical modeling of tectonic fabric, Tectonophysics 197, 295–308, 1991.

[25] R. Hey, F.K. Duennebier and W.J. Morgan, Propagating rifts on mid-ocean ridges, J. Geophys. Res. 85, 3647–3658, 1980.

[26] R.L. Carlson, Late Cenozoic rotations of the Juan de Fuca Ridge and the Gorda Rise: A case study, Tectonophysics 77, 171–188, 1981.

[27] R.N. Hey and D.S. Wilson, Propagating rift explanation for the tectonic evolution of the Northeast Pacific—the pseudomovie, Earth Planet. Sci. Lett. 58, 167–188, 1982.

[28] D.S. Wilson, R.N. Hey and C. Nishimura, Propagation as a mechanism of reorientation of the Juan de Fuca Ridge, J. Geophys. Res. 89, 9215–9225, 1984.

[29] J.L. Karsten, S.R. Hammond, E.E. Davis and R.G. Currie, Detailed geomorphology and neotectonics of the Endeavour Segment, Juan de Fuca Ridge: new results from Seabeam swath mapping, Geol. Soc. Am. Bull. 97, 213–221, 1986.

[30] P.R. Stoddard, A kinematic model for the evolution of the Gorda plate, J. Geophys. Res. 92, 11524–11532, 1987.

[31] D.S. Wilson, Tectonic history of the Juan de Fuca Ridge over the last 40 million years, J. Geophys. Res. 93, 11863–11876, 1988.

[32] E. Davis, R. Currie and B. Sawyer, Acoustic imagery: North Central Juan De Fuca ridge, Geol. Soc. Canada, Ottawa, Canada, 1987.

[33] L.J. Perram, M.-H. Cormier and K.C. Macdonald, Magnetic and tectonic studies of the dueling propagator spreading centers at 20°40'S on the East Pacific Rise: Evidence for crustal rotation, J. Geophys. Res. 98, 13,835–13,850, 1993.

[34] P.R. Shaw, Ridge segmentation, faulting and crustal thickness in the Atlantic Ocean, Nature 358, 490–493, 1992.

[35] J.W. Sinton, D.S. Wilson, D.M. Christie, R.N. Hey and J.R. Delaney, Petrologic consequences of rift propagation on oceanic spreading ridges, Earth Planet. Sci. Lett. 62, 193–207, 1983.